

Theory of a two-level artificial molecule in laterally coupled quantum Hall droplets

Ramin M. Abolfath, W. Dybalski, and Pawel Hawrylak

Institute for Microstructural Sciences, National Research Council of Canada, Ottawa, K1A 0R6, Canada

(Dated: April 1, 2020)

We present a theory of laterally coupled quantum Hall droplets with electron numbers (N_1, N_2) at filling factor $\nu = 2$. We show that the edge states of each droplet are tunnel coupled and form a two-level artificial molecule. By populating the edge states with one electron each a two electron molecule is formed. We predict the singlet-triplet transitions of the effective two-electron molecule as a function of the magnetic field, the number of electrons, and confining potential using the configuration interaction method (CI) coupled with the unrestricted Hartree-Fock (URHF) basis. In addition to the singlet-triplet transitions of a 2 electron molecule involving edge states, triplet transitions involving transfer of electrons to the center of individual dots exist for $(N_1 \geq 5, N_2 \geq 5)$.

PACS numbers: 73.43.Lp

I. INTRODUCTION

There is currently significant experimental^{1,2,3,4,5,6,7,8,9,10,11,12} and theoretical^{13,14,15,16,17,18,19,20,21,22,23} interest in coupled lateral quantum dots. The main effort is on developing means of control of quantum mechanical coupling of artificial molecules, with each dot playing the role of an artificial atom^{5,6,7,13}. This is stimulated largely by the prediction that with one electron in each dot, the magnetic field driven singlet-triplet spin transitions of a two-level molecule have potential application as quantum gates^{15,16,17,19}. Recent experiments by Pioro-Ladriere et al. in Ref.6 suggested that one can create an effective two-level molecule in many electron lateral quantum dots by the application of high magnetic field. In strong magnetic field electrons are expected to form quantum Hall droplet in each quantum dot. Edge states of each droplet can be coupled in a controlled way using barrier electrodes, and at filling factor $\nu = 2$ effectively reduce the many-electron-double dot system to a two-level molecule⁶. When populated with one electron each, one expects to have singlet triplet transitions of two valence electrons in the background of core electrons of the spin singlet $\nu = 2$ droplets. This is schematically illustrated in Fig.1 where lateral lines correspond to energies of orbitals of the lowest Landau level in each droplet as a function of position, with solid lines being occupied by the spin up/down core electrons, and dashed lines by the valence electrons in edge states. In analogy with a single dot^{4,22} the orbitals of the second Landau level of each dot are also shown. The energy of these orbitals becomes comparable to the energy of valence electrons when the number of electrons is ≥ 5 per dot. For these electron numbers it is possible in single dots to move electrons from the edge valence orbitals to 2LL orbitals localized in the center.

These qualitative considerations are supported by a presented here microscopic theory of laterally coupled quantum Hall droplets. The quantum dot molecules studied in this work differ from the single dots by the complex confining potential, and by twice as many elec-

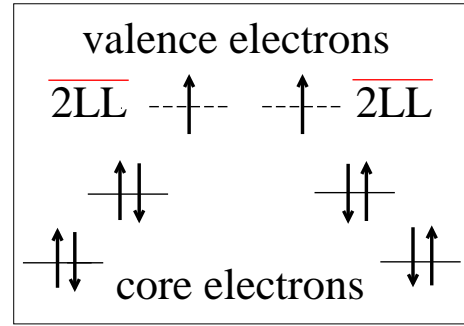


FIG. 1: $\nu = 2$ droplets

trons. We address these difficulties by extending the combination of the Hartree-Fock and exact diagonalization configuration interaction techniques, introduced to study single dots in Ref. 22, to real space calculations for large electron numbers in double dots. This allows us to predict the magnetic field induced singlet-triplet spin transitions of quantum Hall droplets with (N_1+1, N_2+1) electron numbers, interpret them in terms of an effective two-electron (1,1) artificial molecule, and determine exchange coupling constant J as a function of the number of core electrons and the magnetic field. The possibility of storing electrons in 2LL orbitals is demonstrated.

II. HAMILTONIAN

Our theory is based on effective mass envelope function to describe the confined electrons in quantum dots. We consider electron motion to be quasi-two-dimensional and coupled to the perpendicular external magnetic field by vector potential A . With the total number of electrons $N = N_1 + N_2$ the quantum dot molecule Hamiltonian

can be written as:

$$H = \sum_{i=1}^N T_i + \frac{e^2}{2\epsilon} \sum_{i \neq j} \frac{1}{|\vec{r}_i - \vec{r}_j|}, \quad (1)$$

where $T = \frac{1}{2m^*} \left(\frac{\hbar}{i} \nabla + \frac{e}{c} A(\vec{r}) \right)^2 + V(x, y)$ is the one electron Hamiltonian with $V(\vec{r})$ the quantum dot molecule confining potential, m^* the conduction-electron effective mass, e the electron charge, and ϵ the host semiconductor dielectric constant. The Zeeman spin splitting (very small for GaAs) is neglected here. In what follows we use GaAs effective atomic energy and length units with $Ry^* = 5.93meV$, and $a_0^* = 9.79nm$. The choice of gauge A plays significant role in improving the numerical accuracy of single particle spectrum. Because the quantum dot molecules considered in this study are weakly coupled, we adopt a gauge field to separate the vector potential A into two parts: $A = A_L$ if $x < 0$ and $A = A_R$ otherwise. To distinguish the electrons localized in the different dots we use the pseudo-spin labels left (L) and right (R). Here $A_L = (B/2)(-y, x + a)$, and $A_R = (B/2)(-y, x - a)$ are localized vector potentials at the center of each dot, B is the magnetic field, and $2a$ is the inter-dot separation. The associated wavefunctions for electron in the left and right dot are connected via a gauge transformation $\psi_L(\vec{r}) = \psi_R(\vec{r}) \exp(-i\hbar\omega_c \frac{ay}{2})^{25}$.

III. CONFINING POTENTIAL

The double quantum dot potential $V(x, y)$ defined by electrostatic gates is characterized by two potential minima. With our focus on electronic correlations, we parameterize electrostatic potential of a general class of coupled quantum dots by a sum of three Gaussians¹⁹ $V(x, y) = V_L \exp[-\frac{(x+a)^2+y^2}{\Delta^2}] + V_R \exp[-\frac{(x-a)^2+y^2}{\Delta^2}] + V_p \exp[-\frac{x^2}{\Delta_{Px}^2} - \frac{y^2}{\Delta_{Py}^2}]$. Here V_L, V_R describe the depth of the left and right quantum dot minima located at $x = -a, y = 0$ and $x = +a, y = 0$, and V_p is the plunger gate potential controlled by the central gate. For identical dots, $V_L = V_R = V_0$, and confining potential exhibits inversion symmetry. In the following numerical examples we will parameterize it by $V_0 = -10, a = 2, \Delta = 2.5$, and $\Delta_{Px} = 0.3, \Delta_{Py} = 2.5$, in effective atomic units. V_p , which controls the potential barrier, is varied between zero and $10Ry^*$, independent of the locations of the quantum dots. The choice of parameters ensures weakly coupled quantum dots.

IV. SINGLE PARTICLE SPECTRUM

The potential of each isolated dot is a single Gaussian potential. Expanding it in the vicinity of the minimum yields a parabolic potential $V(r) = m^*\omega_0^2 r^2/2$ with the strength $\omega_0 = 2\sqrt{|V_0|}/\Delta^2$. The low energy spectrum of each dot corresponds to two harmonic oscillators with

eigen-energies $\varepsilon_{nm} = \hbar\omega_+(n+1/2) + \hbar\omega_-(m+1/2)$. Here $\omega_{\pm} = \sqrt{\omega_0^2 + \omega_c^2/4} \pm \omega_c/2$, ω_c is the cyclotron energy, and $n, m = 0, 1, 2, \dots$. With increasing magnetic field the $\hbar\omega_-$ decreases to zero while $\hbar\omega_+$ approaches the cyclotron energy ω_c , and the states $|m, n\rangle$ evolve into the n th Landau level. The $\nu = 2$ spin singlet quantum Hall droplet is formed if $2N$ electrons occupy the N successive $|m, n = 0\rangle$ lowest Landau level (LLL) orbitals. When extra $2N + 1$ th electron is added it occupies the edge orbital $|m = N, n = 0\rangle$. These $(2 \times N + 1, 2 \times N + 1)$ configurations, for the two isolated dots, are shown in Fig.1. In each isolated dot increasing the magnetic field leads to spin flips while decreasing the magnetic field lowers the energy of the edge $|m = N, n = 0\rangle$ orbital with respect to the lowest unoccupied center orbital $|m = 0, n = 1\rangle$ of the second Landau level (2LL). At a critical magnetic field a LL crossing occurs and the electron transfers from the edge orbital to central orbital, leading to redistribution of electrons from the edge to center.^{4,22}

We now turn to the description of coupled dots in strong magnetic field ($n = 0$). As a first approximation one might expect the $|m; L\rangle$ orbitals of the left dot L to be coupled only with the corresponding $|m; R\rangle$ orbitals of the right (R) dot, and form a pair of the symmetric and anti-symmetric orbitals

$$|m, \pm\rangle = \frac{1}{\sqrt{2(1 \pm S_m)}} (|m, L\rangle \pm |m, R\rangle), \quad (2)$$

where $S_m = Re(\langle m, L | m, R \rangle)$. Therefore in high magnetic field we expect the formation of shells of closely spaced pairs of bonding-antibonding levels. This is illustrated in Fig. 2 which shows the magnetic field evolution of the numerically calculated single particle spectrum of a double dot. For the illustration we scale the unit of energy by $\hbar\omega_0 \approx 2.53Ry^*$, using the parameters of the confinement potential with the energy barrier set to $V_p = 7Ry^*$. The single particle eigenvalues and eigenvectors calculated by diagonalizing T are given by $\tilde{\epsilon}_j$ and $\tilde{\varphi}_j$ respectively. The spectrum is calculated accurately by discretizing in real space the single particle Hamiltonian T using special gauge transformation. The resulting large matrices are diagonalized using conjugate gradient algorithms²⁵.

At zero magnetic field Fig. 2 shows the formation of hybridized S, P, and D shells, to be discussed elsewhere²⁵. In high magnetic field the pairs of closely spaced levels $|m, \pm\rangle$ separated by $\approx \omega_-$ are clearly visible. The energy spacing between the levels in each pair increases at higher energy part of spectrum, because the potential barrier is less effective and tunneling becomes stronger.

The existence of pairs of levels in the numerically obtained spectrum suggests that the corresponding wavefunction $|\tilde{\varphi}_j\rangle$ does indeed admit a description in terms of orbitals localized in each dot. This is confirmed by the calculated overlaps $\langle \tilde{\varphi}_j | m, \pm \rangle$ shown in Table I as well as by the corresponding probability densities shown in Fig.3.

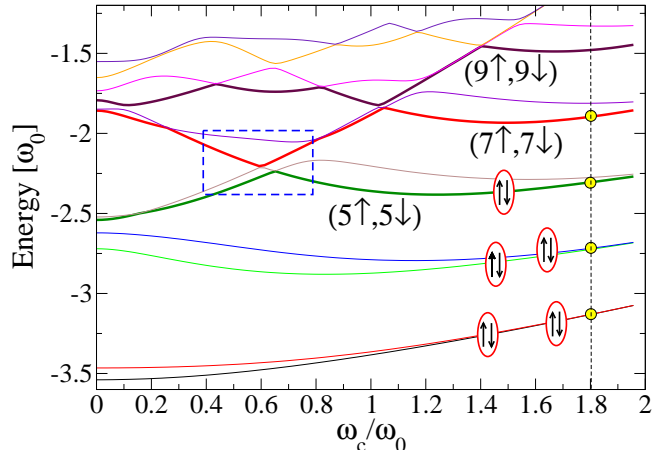


FIG. 2: Double dot single particle spectrum vs. cyclotron energy. Molecular states can be grouped by their parity (or pseudo-spin quantum number \pm). States with j =odd (even) have positive (negative) parity (pseudo-spin). States with opposite parity cross and states with the same parity anticross. An enlarged part of spectrum, inside the box surrounded by the dashed lines, is shown in Fig. 4.

| $\omega_c = 1.8\omega_0$ | $\tilde{\epsilon}_j[\omega_0]$ | $\epsilon_{LCAO}[\omega_0]$ |
|----------------------------------|--------------------------------|-----------------------------|
| $ \langle 1 1+\rangle ^2 = 0.99$ | -3.13 | -3.12 |
| $ \langle 2 1-\rangle ^2 = 0.99$ | -3.12 | -3.12 |
| $ \langle 3 2+\rangle ^2 = 0.98$ | -2.72 | -2.71 |
| $ \langle 4 2-\rangle ^2 = 0.99$ | -2.71 | -2.70 |
| $ \langle 5 3+\rangle ^2 = 0.95$ | -2.30 | -2.28 |
| $ \langle 6 3-\rangle ^2 = 0.99$ | -2.27 | -2.26 |

TABLE I: Comparison between real space molecular wave functions $|\tilde{\varphi}_j\rangle$ and the linear combination atomic orbitals (LCAO) $|m\pm\rangle$ is given by the overlap $|\langle \tilde{\varphi}_j|m\pm\rangle|^2$ at $\omega_c = 1.8\omega_0$. The corresponding energies are shown.

An important part of the single particle spectrum is the $\nu = 2$ phase where electrons with opposite spin occupy the first Landau level orbitals (in weak Zeeman coupling limit). In a Fock-Darwin picture of a quantum dot spectrum, this corresponds to the $|m, n = 0\rangle$ orbitals just after the last orbital crossing with the $|m = 0, n = 1\rangle$ orbital. In coupled quantum dots, we are interested in transitions between the states derived from the lowest Landau level and the states derived from the second Landau level. The crossing of the two levels in a single dot can occur for the 3rd and higher levels. A similar effect takes place in a coupled quantum dot but for the fifth and higher levels. The single-electron probability density of the 5th level at $\omega_c = 0.5\omega_0$ and at $\omega_c = 0.8\omega_0$ is shown in Fig. 4. The electron which occupies the 5th level is closer to the center of each dot at low magnetic fields. It then moves to an edge configuration at higher fields.

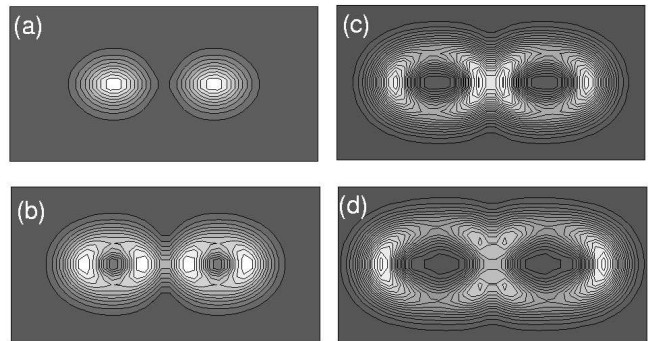


FIG. 3: Single electron densities at $\omega_c = 1.8\omega_0$ corresponding to $j = 1, 3, 5$, and $j = 7$ (from a to d).

From the single particle spectrum presented in Fig. 2, the first set of electronic configurations which probe such crossing consists of 9-12 electrons occupying five lowest single particle states. The corresponding (5,5) half-filled shell configuration is shown in Fig.2. The characteristic shell structure of a coupled dot in high magnetic field leads to magnetic electron numbers populating different $|m, \pm\rangle$ electronic shells. The half-filled shells correspond to electron numbers $(N1, N2) = (1, 1), (3, 3), (5, 5), (7, 7), \dots$ while filled shells correspond to $(N1, N2) = (2, 2), (4, 4), (6, 6), (8, 8), \dots$ configurations. We expect the half and fully filled shells to have special electronic properties. In particular, the half filled shells offer the possibility of singlet-triplet transitions. For the shells (5,5) and up we expect to be able to move the valence electrons from the edge orbitals to the center orbitals. The crossing of the edge and center orbitals is visible as a cusp in the energy of the fifth molecular orbital shown as a bold line in Fig.2.

V. MANY BODY SPECTRUM

We now turn to the effect of electron-electron interactions. Denoting the creation (annihilation) operators for electrons in non-interacting SP state $|\alpha\sigma\rangle$ by $\tilde{c}_{\alpha\sigma}^\dagger$ ($\tilde{c}_{\alpha\sigma}$), the Hamiltonian of an interacting system in second quantization can be written as

$$H = \sum_{\alpha\beta} \sum_{\sigma\sigma'} \langle \alpha\sigma|T|\beta\sigma'\rangle \tilde{c}_{\alpha\sigma}^\dagger \tilde{c}_{\beta\sigma'} + \frac{1}{2} \sum_{\alpha\beta\gamma\mu} \sum_{\sigma\sigma'} \tilde{V}_{\alpha\sigma,\beta\sigma',\gamma\sigma',\mu\sigma} \tilde{c}_{\alpha\sigma}^\dagger \tilde{c}_{\beta\sigma'}^\dagger \tilde{c}_{\gamma\sigma'} \tilde{c}_{\mu\sigma}, \quad (3)$$

where $\langle \alpha\sigma|T|\beta\sigma'\rangle = \tilde{\epsilon}_{\alpha\sigma} \delta_{\alpha\beta} \delta_{\sigma\sigma'}$ and $\tilde{V}_{\alpha\sigma,\beta\sigma',\mu\sigma',\nu\sigma} = \int d\vec{r} \int d\vec{r}' \tilde{\varphi}_{\alpha\sigma}^*(\vec{r}) \tilde{\varphi}_{\beta\sigma'}^*(\vec{r}') \frac{e^2}{\epsilon|\vec{r}-\vec{r}'|} \tilde{\varphi}_{\mu\sigma'}(\vec{r}') \tilde{\varphi}_{\nu\sigma}(\vec{r})$, are the

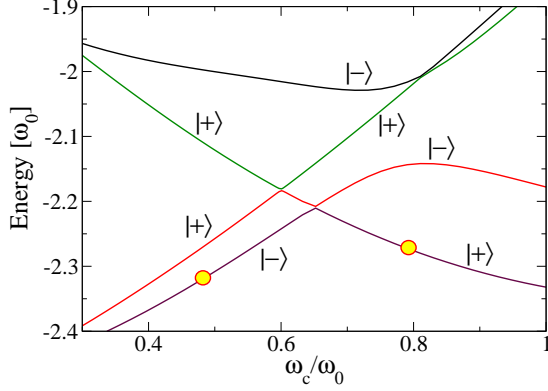


FIG. 4: Top: Energies of single particle states with their parities are shown. States with positive and negative parities are represented by pseudo-spin indices $|\pm\rangle$. Bottom: The 5th single-particle orbital between two sides of Landau level crossing is shown at $\omega_c = 0.5\omega_0$, and $\omega_c = 0.8\omega_0$. The top and bottom correspond to the innermost orbital of second Landau level and outermost of the first Landau level.

single particle and the two-body Coulomb matrix elements. Here α, β, μ, ν are spatial orbital indices, and σ, σ' are the spin indices. $\tilde{\epsilon}_{\alpha\sigma}$ is the single particle energy, e is the electric charge.

A. Unrestricted Hartree-Fock Approximation (URHFA)

We now proceed to include electron-electron interactions in two steps: direct and exchange interaction using unrestricted Hartree-Fock approximation (URHF), and correlations using URHF basis in the configuration interaction method (URHF-CI). The spin-dependent HF

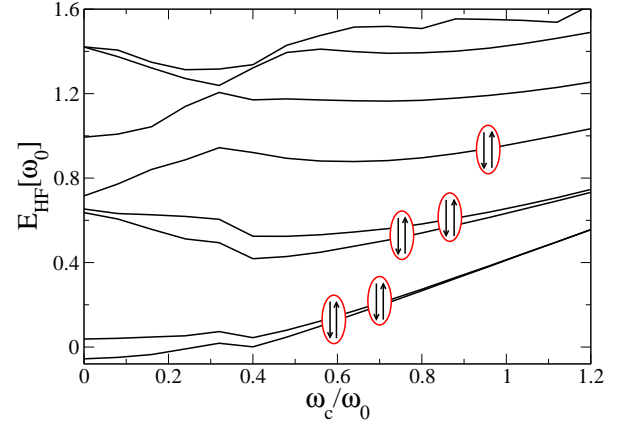


FIG. 5: URHF eigen-energies vs. cyclotron energy for 10 electrons. The HF energy gap between HOMO (highest occupied molecular orbital), and LUMO (lowest unoccupied molecular orbital) is clearly visible.

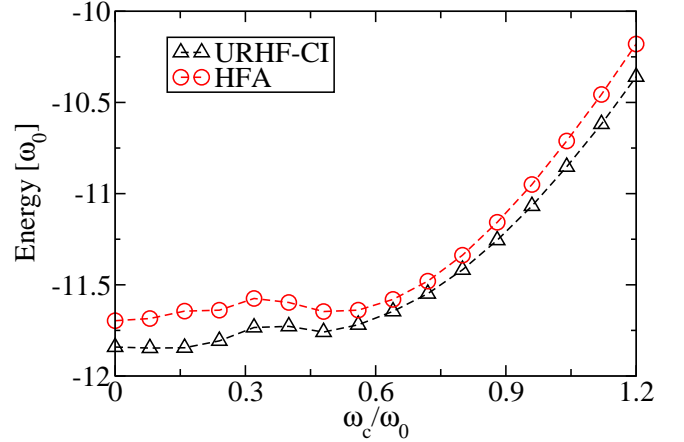


FIG. 6: URHFA, and URHFA-CI ground state energy vs. cyclotron energy are shown for a quantum dot molecule.

orbitals $|\varphi_{i\sigma}\rangle$ are obtained from the N_l non-interacting single particle orbitals $|\tilde{\varphi}_\alpha\rangle$, energy spectrum of which is shown in Fig.2, by the transformation $|\varphi_{i\sigma}\rangle = \sum_{\alpha=1}^{N_l} a_{\alpha\sigma}^{(i)} |\tilde{\varphi}_\alpha, \sigma\rangle$. The variational parameters $a_{\alpha\sigma}^{(i)}$ are solutions of self-consistent Pople-Nesbet equations²⁴:

$$\sum_{\gamma=1}^{N_l} \{\tilde{\epsilon}_\mu \delta_{\gamma\mu} + \sum_{\alpha,\beta=1}^{N_l} \tilde{V}_{\mu\alpha\beta\gamma} [\sum_{j=1}^{N_\uparrow} a_{\alpha\uparrow}^{*(j)} a_{\beta\uparrow}^{(j)} + \sum_{j=1}^{N_\downarrow} a_{\alpha\downarrow}^{*(j)} a_{\beta\downarrow}^{(j)}] - \tilde{V}_{\mu\alpha\gamma\beta} \sum_{j=1}^{N_\uparrow} a_{\alpha\uparrow}^{*(j)} a_{\beta\uparrow}^{(j)}\} a_{\gamma\uparrow}^{(i)} = \epsilon_{i\uparrow} a_{\mu\uparrow}^{(i)}, \quad (4)$$

where $\tilde{V}_{\alpha\beta\mu\nu}$ are Coulomb matrix elements calculated using non-interacting single particle states. A similar equation holds for spin down electrons. The calculations are carried out for all possible total spin S_z configurations. The calculated HF eigen-energies and total energies for the $N = 10$ electrons with $S_z = 0$ in a magnetic field are shown in Figs. 5 and 6. Comparing HF spectrum (Fig. 5) with the single particle spectrum (Fig. 2), one observes that a HF gap developed at the Fermi level, between the highest occupied molecular state, and the lowest unoccupied molecular state, and the Landau level crossing between single particle Landau levels has been shifted to lower magnetic fields, from $\omega_c = 0.6\omega_0$ in single particle spectrum to $\omega_c = 0.3\omega_0$ in HF spectrum.

B. URHF configuration interaction method

Correlations are included via configuration interaction method. Denoting the creation (annihilation) operators for URHF quasi-particles by c_i^\dagger (c_i) with the index i representing the combined spin-orbit quantum numbers, the many body Hamiltonian of the interacting system can be written as:

$$H = \sum_{ij} \langle i|T|j \rangle c_i^\dagger c_j + \frac{1}{2} \sum_{ijkl} V_{ijkl} c_i^\dagger c_j^\dagger c_k c_l, \quad (5)$$

where $\langle i|T|j \rangle = \epsilon_i S_{ij} - \langle i|V_H + V_X|j \rangle$, V_{ijkl} are the Coulomb matrix elements in the URHF basis, ϵ_i are the URHF eigenenergies, V_H and V_X are the Hartree and exchange operators, and $S_{ij} \equiv \langle \varphi_i | \varphi_j \rangle$ are the spin up and spin down orbitals overlap matrix elements. The Hamiltonian matrix is constructed in the basis of configurations, and diagonalized using conjugated gradient methods for different total S_z . The convergence of CI calculation for the (5,5) droplets has been checked by increasing the URHF basis up to $N_S = 20$, associated with 240 374 016 configurations. Fig. 6 shows the ground state energy for $N = 10$ electrons as a function of magnetic field obtained using URHF and URHF-CI methods. The inclusion of correlations lowers total energy by $\approx 0.4Ry^*$ at $\omega_c = 0$ to $0.3Ry^*$ at $\omega_c = 0.9\omega_0$. The results of calculated exchange interaction $J \equiv E_{\text{triplet}} - E_{\text{singlet}}$ of the half filled shells (1,1), (3,3), (5,5)-droplets in magnetic field are shown in Fig. 7. The spin singlet-triplet transition at $\omega_c = 0.8\omega_0$ in (5,5)-molecule is equivalent to the magnetic field induced singlet-triplet transition in a two-electron double dot^{17,19,23}. The spin singlet-triplet transition at $\omega_c \approx 0.4\omega_0$ is associated with degeneracy of the LLL edge and 2LL center orbitals. The high magnetic field part of J is quantitatively similar regardless of the number of electrons occupying quantum dots. In small magnetic field single particle states show complex structure which involves Landau level crossings and anti-crossings. It turns out that the dependence of J on the magnetic field is affected by the single particle states of valence and core electrons, which explains the strong de-

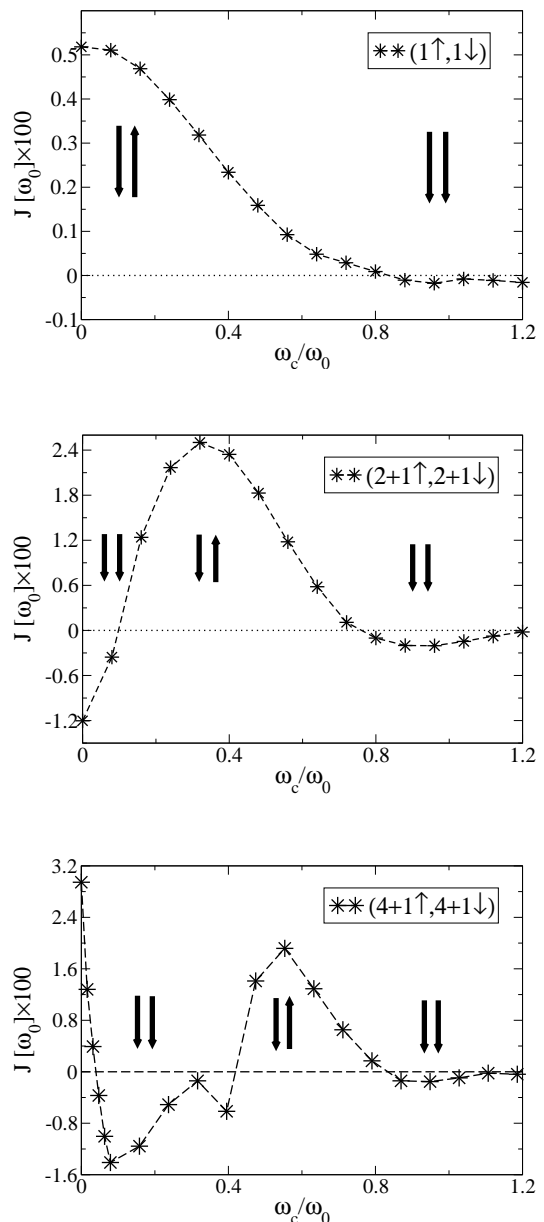


FIG. 7: The energy difference J between the triplet and the singlet ground states of the (1,1), (2+1,2+1), and (4+1,4+1) quantum Hall droplets from URHF-CI as a function of cyclotron energy ω_c .

pendence of J on the electron numbers in low magnetic fields.

VI. CONCLUSIONS

We present here a microscopic theory of laterally coupled quantum Hall droplets with electron numbers (N_1, N_2) at filling factor $\nu = 2$. Using unrestricted Hartree-Fock orbitals as the basis in the configuration-

interaction calculation we have shown that these strongly coupled quantum dots behave effectively as the two-level molecule. When the two-level molecule is populated with two electrons, singlet-triplet spin transition can be induced by the application of high magnetic field. The dependence on the magnetic field and the number of core electrons of the singlet-triplet gap J has been calculated. It was shown that in ($N1 \geq 5$, $N2 \geq 5$) molecule the valence electrons can be transferred from edge to center states of individual dots. This might offer a possibility of performing quantum operations on valence electrons in

edge states and storage in center orbitals.

VII. ACKNOWLEDGEMENT

M.A. and P.H. acknowledge support by the NRC High Performance Computing project. P.H. acknowledges support by Canadian Institute for Advanced Research and W. D. acknowledges support by NSERC. Authors thank A.Sachrajda and M.Pioro-Ladriere for discussions.

-
- ¹ C. Livermore, C. H. Crouch, R. M. Westervelt, K. L. Campman, A. C. Gossard, *Science* **274**, 1332 (1996).
- ² T. H. Oosterkamp, T. Fujisawa, W. G. Van Der Wiel, K. Ishibashi, R. V. Hijman, S. Tarucha, and L. P. Kouwenhoven, *Nature (London)* **395**, 873 (1998); T. H. Oosterkamp, S. F. Godijn, M. J. Uilenreef, Y. V. Nazarov, N. C. van der Vaart, and L. P. Kouwenhoven, *Phys. Rev. Lett.* **80**, 4951 (1998).
- ³ Alexander W. Holleitner, Robert H. Blick, Andreas K. Huttel, Karl Eberl, and Jorg P. Kotthaus, *Science* **297**, 70 (2001).
- ⁴ M. Ciorga, A. Wensauer, M. Pioro-Ladriere, M. Korkusinski, J. Kyriakidis, A. S. Sachrajda, and P. Hawrylak, *Phys. Rev. Lett* **88**, 256804 (2002).
- ⁵ W. G. van der Wiel, S. De Franceschi, J. M. Elzerman, T. Fujisawa, S. Tarucha, L. P. Kouwenhoven, *Rev. Mod. Phys.* **75**, 1 (2003).
- ⁶ M. Pioro-Ladriere, M. Ciorga, J. Lapointe, P. Zawadzki, M. Korkusinski, P. Hawrylak, and A. S. Sachrajda, *Phys. Rev. Lett.* **91**, 026803 (2003).
- ⁷ J.R. Petta, A. C. Johnson, C. M. Marcus, M. P. Hanson, and A. C. Gossard, *Phys. Rev. Lett.* **93**, 186802 (2004).
- ⁸ M. Rontani, S. Amaha, K. Muraki, F. Manghi, E. Molinari, S. Tarucha, and D. G. Austing, *Phys. Rev. B* **69**, 085327 (2004).
- ⁹ J. R. Petta, A. C. Johnson, C. M. Marcus, M. P. Hanson, and A. C. Gossard *Phys. Rev. Lett.* **93**, 186802 (2004).
- ¹⁰ N. J. Craig, J. M. Taylor, E. A. Lester, C. M. Marcus, M. P. Hanson, and A. C. Gossard, *Science* **23** (2004).
- ¹¹ T. Hatano, M. Stopa, T. Yamaguchi, T. Ota, K. Yamada, and S. Tarucha, *Phys. Rev. Lett.* **93**, 066806 (2004).
- ¹² M. Pioro-Ladriere, M. R. Abolfath, P. Zawadzki, J. Lapointe, S. A. Studenikin, A. S. Sachrajda, and P. Hawrylak, *Phys. Rev. B* **72**, 125307 (2005).
- ¹³ J. J. Palacios and P. Hawrylak, *Phys. Rev. B* **51**, 1769 (1995).
- ¹⁴ M. Koskinen, M. Manninen, and S.M. Reimann, *Phys. Rev. Lett.* **79**, 1389 (1997).
- ¹⁵ J. A. Brum, and P. Hawrylak, *Superlattices Microstruct.* **22**, 431 (1997).
- ¹⁶ D. Loss and D. P. DiVincenzo, *Phys. Rev. A* **57**, 120 (1998).
- ¹⁷ G. Burkard, D. Loss and D. P. DiVincenzo, *Phys. Rev. B* **59**, 2070 (1999).
- ¹⁸ A. Wensauer, O. Steffens, M. Suhrke, and U. Rössler, *Phys. Rev. B* **62**, 2605 (2000).
- ¹⁹ Xuedong Hu and S. Das Sarma, *Phys. Rev. A* **64**, 042312 (2001).
- ²⁰ C. Yannouleas and U. Landman, *Phys. Rev. Lett.* **82**, 5325 (1999); Constantine Yannouleas and Uzi Landman, *Phys. Rev. B* **68**, 035326 (2003)
- ²¹ A. Harju, S. Siljamki, and R. M. Nieminen, *Phys. Rev. Lett.* **88**, 226804 (2002).
- ²² A. Wensauer, M. Korkusinski, P. Hawrylak, *Phys. Rev. B* **67**, 035325, (2003).
- ²³ W. Dybalski, and P. Hawrylak, *Phys. Rev. B* **72**, 205432 (2005).
- ²⁴ A. Szabo and N. S. Ostlund, *Modern Quantum Chemistry* (McGraw-Hill, New York, 1989).
- ²⁵ R. M. Abolfath, P. Hawrylak, cond-mat/0511741.